The Astronomical Journal, ACCEPTED
Preprint typeset using LaTeX style emulateapj v. 5/2/11

SLoWPoKES-II: 100,000 WIDE BINARIES IDENTIFIED IN SDSS WITHOUT PROPER MOTIONS

SAURAV DHITAL [1,2,3], ANDREW A. WEST [2], KEIVAN G. STASSUN [3,4], KYLE J. SCHLUNS [2], ANGELA P. MASSEY [2]

Submitted: January 11, 2015; accepted: April 16, 2015; published:

ABSTRACT

We present the SLoWPoKES–II catalog of low-mass visual binaries identified from the Sloan Digital Sky Survey by matching photometric distances. The candidate pairs are vetted by comparing the stellar density at their respective Galactic positions to Monte Carlo realizations of a simulated Milky Way. In this way, we are able to identify large numbers of bona fide wide binaries without the need of proper motions. 105,537 visual binaries with angular separations of $\sim$1–20$''$, are identified, each with a probability of chance alignment of $\leq$5%. This is the largest catalog of bona fide wide binaries to date, and it contains a diversity of systems—in mass, mass ratios, binary separations, metallicity, and evolutionary states—that should facilitate follow-up studies to characterize the properties of M dwarfs and white dwarfs. There is a subtle but definitive suggestion of multiple populations in the physical separation distribution, supporting earlier findings. We suggest that wide binaries are comprised of multiple populations, most likely representing different formation modes. There are 141 M7 or later wide binary candidates, representing a 7-fold increase in the number currently known. These binaries are too wide to have been formed via the ejection mechanism. Finally, we find that $\sim$6% of spectroscopically confirmed M dwarfs are not included in the SDSS STAR catalog; they are misclassified as extended sources due to the presence of a nearby or partially resolved companion. The SLoWPoKES–II catalog is publicly available to the entire community on the world wide web via the Filtergraph data visualization portal.

Subject headings: (stars:) binaries: visual — stars: low mass — stars: brown dwarfs — stars: late-type — (stars:) white dwarfs — (stars:) subdwarfs stars: statistics —

1. INTRODUCTION

Components of binary (or multiple) systems are ideal coeval laboratories to study star formation, to benchmark stellar evolutionary models, and to calibrate empirical relations that determine fundamental stellar parameters. While detailed and precise measurements of individual objects or small samples provide important tests for evolutionary models (e.g., White et al. 1999; Stassun et al. 2007, 2008), large statistical samples are necessary for properly constraining the behavior and intrinsic variation of star formation and of stellar properties. All of these rest on the premise that individual components in a stellar system are formed at the same time (White & Ghez 2001; Kraus & Hillenbrand 2009a), of the same material (Schuler et al. 2011; Dhital et al. 2012), and have evolved in the same environment.

Until recently, the intrinsic faintness of low-mass stars—generally defined as the regime bracketed by the hydrogen burning minimum mass, $\sim$0.075 $M_\odot$ (Burrows et al. 1997), and the onset of molecular lines in the photosphere, $\sim$0.8 $M_\odot$ (Kirkpatrick et al. 1991)—has limited studies to small, nearby samples. Almost two decades ago, the Palomar–Michigan State University (PMSU) survey cataloged the spectra for $\sim$3,000 M dwarfs (dMs) and was the largest such study (Reid et al. 1995; Hawley et al. 1996). Other samples used to study the distribution of low-mass binaries and to calibrate low-mass stellar properties using binaries were even smaller, with 30–100 systems (Fischer & Marcy 1992; Henry & McCarthy 1993; Reid & Gizis 1997; Delfosse et al. 2004). Hence, these studies often lacked the statistical robustness for firm, independent results, which were then often tethered to and studied in comparison with higher-mass stars. In addition, modeling efforts for the low-mass late-K and M dwarfs have been stymied by incomplete molecular line lists resulting in uncertain opacities caused by the molecules in the stellar photosphere at effective temperatures of $\lesssim$4300 K (Hauschildt, Allard, & Baron 1999). As a result of these observational and modeling challenges, low-mass stars have not been well characterized, and our techniques for measuring their properties are ill-defined. However, low-mass stars comprise of $\gtrsim$70% of the stars in the Galaxy (Henry 1998) and are the best tracers of its distribution and (at least nearby) structure (e.g. Bochanski et al. 2010). Low-mass stars also have lifetimes longer than that of the Galaxy (Laughlin et al. 1997), making them the ideal tracers of its formation, chemical, and dynamical history.

The advent of deep, all-sky surveys has revolutionized low-mass star and brown dwarf science. In particular, the Sloan Digital Sky Survey (SDSS; York et al. 2000), the Two Micron All Sky Survey (2MASS; Cutri et al. 2003), and UKIRT Infrared Deep Sky Survey (UKIDSS; Lawrence et al. 2007), and Wide-field Infrared Survey Explorer (e.g., Wright et al. 2010) have been critical in expanding sample sizes. SDSS alone has enabled a photometric catalog of >30 million (Bochanski et al. 2010) and spectroscopic catalog of >70,000 (West et al. 2011, hereafter, W11) low-mass stars. Munn et al. (2004, 2008) combined the USNO-B and SDSS astrometry to calculate proper motions for SDSS photometric catalogs. This proper motion catalog is 90% complete down to $g < 19.7$, with typical errors of 5–7mas yr^{-1}. However, the lower resolution limits the catalog to sources separated by $\sim 7''$.

Dhital et al. (2010, hereafter, Paper I) identified the Sloan Low-mass Wide Pairs of Kinematically Equivalent Stars

[1] Department of Physical Sciences, Embry–Riddle Aeronautical University, 600 South Clyde Morris Blvd., Daytona Beach, FL 32114, USA; dhitals@erau.edu
[2] Department of Astronomy, Boston University, 725 Commonwealth Avenue, Boston, MA 02215, USA.
[3] Department of Physics & Astronomy, Vanderbilt University, 6301 Stevenson Center, Nashville, TN, 37235, USA
[4] Department of Physics, Fisk University, 1000 17th Avenue N., Nashville, TN 37208, USA.

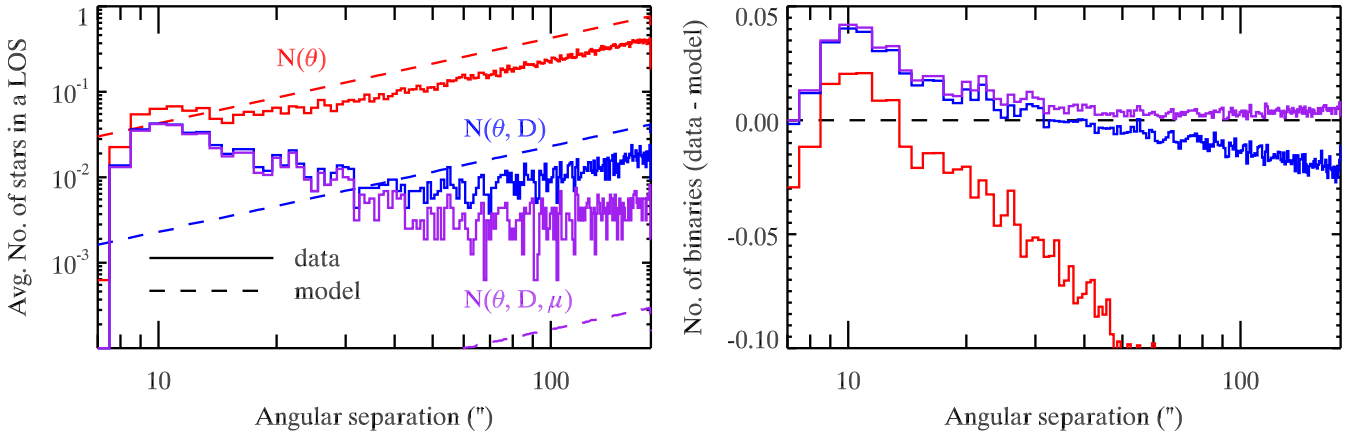

Figure 1. The average number of visual companions (left) and real binaries (right), as assessed by our Galactic models, as a function of angular separation in >1600 lines-of-sight where binary candidates were identified in the SLoWPoKES catalog (Paper I). The solid histograms shows the SDSS distributions while the dashed histograms show the distributions generated in our Monte Carlo models. In this figure, we show the distribution of the average number of companions around $\gtrsim$1600 candidates. We succesively match the angular separation (with the results shown in red histograms), photometric distances (blue), and proper motions (purple). The model distributions predict more stars at larger angular separations as they include all stars whereas the data count only the stars that are detected in SDSS. Intriguingly, the blue and purple histograms were almost identical up to 20–25″, suggesting proper motions were not needed to identify those binaries. This is seen even more clearly in the right panel. In this paper, we conduct a search for binary companions around ∼24 million low-mass stellar sources in the SDSS survey without using proper motions.

(SLoWPoKES) catalog of wide binaries by matching positions, photometric distances, and vector proper motions. The fidelity of each pair was assessed by a six-dimensional Galactic model, which was built using empirical stellar number density (Jurić et al. 2008; Bochanski et al. 2010) and space velocity distributions (Bochanski et al. 2007). With 1342 common proper motion pairs, with $\leq$5% probability of chance alignments, SLoWPoKES was the largest catalog of low-mass, wide binaries and contained a diverse set of pairs with G/K+dM, white dwarf (WD)+dM, dM+dM, and M subdwarf (sdM+sdM) systems. SLoWPoKES has enabled a variety of follow-up observations to probe higher-order multiplicity (Law et al. 2010), metallicity (Dhital et al. 2012), activity (Gunning et al. 2014), rotation, and the age–activity relation (Morgan et al., *in preparation*, Massey et al., *in preparation*) of M dwarfs. In addition, (Andrews et al. 2012, 2015) have adapted the technique used for SLoWPoKES to identify double the sample of known wide WD+WD binaries.

The SLoWPoKES catalog was restricted at small angular separations ($\theta \leq 7''$) and at lower masses ($\lesssim$ M6) by its dependence on the SDSS/USNO-B proper motions (Munn et al. 2004). Specifically, due to the shallow faintness limit of USNO-B, a significant fraction of mid–late dMs that are detected in SDSS do not have USNO-B counterparts and, therefore, proper motions. Similarly, the resolution of USNO-B sets a separation limit of $\sim 7''$ for the SDSS/USNO-B proper motion catalog. These incompleteness are inherited by the SLoWPoKES catalog. In addition, using proper motions to identify binaries precludes systems that are either at large distances or nearby but moving slowly with respect to the Local Standard of Rest. For example, we used a minimum proper motion of 40 mas yr^{-1} for the SLoWPoKES catalog.

Results from the Galactic model indicated that visual binaries with small angular separations could be identified at a high level of fidelity by matching photometric distances alone (Paper I). Figure 1 (left) shows Figure 5 from Paper I. The solid red histogram shows the number of stars, averaged among $gtrsim$1600 lines-of-sight where binary candidates were identified, as a function of angular separation, as measured in the SDSS DR7 photometric catalog. The dashed red histogram shows the distribution for single, non-associated stars in the same fields as simulated by our Galactic model. In essence, this was a measure of the likelihood of whether the companion stars were real binaries or simply chance alignments. The blue and purple histograms show the distribution when the photometric distances and proper motions were matched. Each addition of a dimension resulted in a rejection of a large number of chance optical pairs. The larger stellar number counts at large separations in our simulations (as compared to the data) was caused largely by the fact that the data were limited to $r \lesssim 20.5$ as the SDSS/USNO-B proper motions were required whereas our Galactic model simulates *all* stellar objects. Two features stood out in this figure: (1) the excess of pairs at small separations, which was how Michell (1767) first identified binary systems, or "double" stars as he called them and (2) the blue and purple histograms were essentially the same until about $\theta \sim 20 - 25''$, suggesting those binaries could have been identified without proper motions. This is even more evident in the right panel of Figure 1, where we have plotted the difference between the data and model distributions. These figures clearly demonstrate that proper motions are not required to identify binaries up to a critical separations with a high level of fidelity. A caveat is that the critical angular separation obviously depends on the magnitude limit of the sample. For the SLoWPoKES sample with a limiting magnitude of $r = 20.5$ and proper motion >40 mas yr^{-1}, >90% of the binary candidates within $20''$ with matching photometric distances also had matching proper motions and were classified as CPM pairs.

In this paper, we extend the SLoWPoKES catalog by identifying binary systems with angular separations of 1–$20''$ based entirely on SDSS photometry and astrometry. This allows us to identify visual binaries to $r = 22.2$, with significant numbers at the mid–late M spectral types. In Section 2 we describe the initial sample of low-mass stars that we search around. As in Paper I, our search algorithm is based on matching angular separation and photometric distances supplemented by a Monte Carlo-based Galactic model, which is described in Section 3. We discuss the characteristics of the resultant binary sample in Section 4. We examine the currently debated formation theories for wide stellar binaries and VLM/BDs in light of SLoWPoKES-II sample of binaries in Section 5. We

summarize our results in Section 6.

The SLoWPoKES and SLoWPoKES-II catalogs, along with followup spectra, are publicly available online.[5].

2. SDSS DATA

One of the largest and most influential astronomical surveys ever conducted to date, SDSS is a comprehensive imaging and spectroscopic survey (York et al. 2000). Over eight years of operation between 2000-2008, it collected imaging and spectroscopic data for over a decade years using a dedicated 2.5-m telescope at Apache Point Observatory, New Mexico (Gunn et al. 2006). The telescope has a 120 megapixel camera that has a field of view of 1.5 square degrees (Gunn et al. 1998) and conducts imaging in five broad optical bands ($ugriz$) between ∼3,000 and 10,000 $\AA$ (Fukugita et al. 1996). The last data release with imaging data, Data Release 8 (DR8), comprised of ∼450 million unique objects over 14,555 square degrees of the sky, spanning the entire northern sky as well as the Southern Galactic Cap (Aihara et al. 2011). The global absolute astrometric precision was 70 mas (Pier et al. 2003) while the photometry has relative calibration accuracies of 2% in the u band and 1% in the $griz$ bands (Padmanabhan et al. 2008). The catalog is 95% complete for point sources of 22.0, 22.2, 22.2, 21.3, and 20.5 in the $ugriz$ bands, respectively (Gunn et al. 1998). The corresponding spectroscopic survey has obtained ∼1.8 million optical spectra, with $\lambda/\Delta\lambda \approx 2000$, over 9274 square degrees (Aihara et al. 2011) using a pair of fiber-fed double spectrographs. The Third Sloan Digital Sky Survey (SDSS-III; Eisenstein et al. 2011), which is comprised of four different spectroscopic surveys, is currently underway.

The DR8 photometric catalog has more than 200 million point sources. As in Paper I, we used the Catalog Archive Server query tool (CasJobs[6]) to select the sample of low-mass stars from the DR8 STAR table as having $r - i \geq 0.3$ and $i - z \geq 0.2$, consistent with spectral types of K5 or later (West et al. 2008). Selecting from the STAR ensures that the object is a PRIMARY and not a duplicate detection and that its morphology is consistent with being a point source. This morphological classification is >95% accurate up to $r \approx 21.5$ (Lupton et al. 2001). Even up to $r \approx 22.5$, stars outnumber galaxies >8:1 (Fadely et al. 2012), and, therefore, we do not expect compact galaxies as frequent interlopers in our sample. To ensure excellent photometry, we made cuts on the standard quality flags—all of PEAKCENTER, NOTCHECKED, PSF_FLUX_INTERP, INTERP_CENTER, BAD_COUNTS_ERROR, SATURATED were set to be 0 (Bochanski et al. 2010; Paper I)—and required the errors in PSF magnitudes to be ≤ 0.10. Throughout our analysis, these quality cuts were performed only for the bands that were used in the analysis for that particular star: iz for M7 or later stars, riz for K5–M7 stars, $griz$ for F0–K5 stars, and $ugriz$ for white dwarfs. While no faintness limits were specifically adopted, the requirement on the error in PSF magnitudes effectively limits resulting samples to the SDSS 95% completeness limits.

The resulting sample yielded 33,589,670 stellar sources, with colors consistent with K5–M9 dwarfs. In Dhital et al. (2010) we found that chance alignments were unacceptably high near the Galactic Plane due to the higher stellar density and the higher uncertainties caused by higher extinction. Therefore, we rejected stars at Galactic latitudes less than 20°. We also rejected stars with photometric distances larger than 2500 pc as the distance uncertainties are larger than ∼350 pc, making distance matching meaningless at those distances (see Section 3.2 for further discussion). As a result, we started with an initial sample of 24,036,982 low-mass stars., around which to search for companions.

[5] http://slowpokes.vanderbilt.edu

[6] http://skyserver.sdss3.org/CasJobs/

3. METHOD: IDENTIFYING BINARY CANDIDATES

3.1. *Assessing the SDSS source classification algorithm*

The tighest binary we were able to identify was $\gtrsim 1''$ (see Figure 7 below), suggesting a fundamental limitation in our technique at that value. However, with a plate scale of $0''.396$ pixel^{-1}, SDSS should be able to distinguish tighter binaries. Both unresolved and partially-resolved binaries, with separations smaller than the resolution limit or the plate scale, have been identified from both the 2MASS (Kraus & Hillenbrand 2007b) and the Palomar Transient Factory (Terziev et al. 2013) photometric catalogs, albeit aided by multi-epoch data in the latter case. Therefore, we conducted an examination of (1) what was restricting us from identifying binaries at $<1''$ and (2) what fraction of resolved binaries we were missing in our resultant sample due to this limitation.

First, we briefly describe the SDSS point source classification scheme. The algorithm is fully documented on the SDSS webpages[7] and is beyond the scope of this paper, thus we only outline the scheme that classifies identified sources into the STAR table. The SDSS pipeline uses RESOLVE to identify unique sources and and DEBLEND to deblend them when multiple sources are present. All of the identified sources, for which photometric parameters have been measured, are cataloged in the PHOTOOBJALL table. This table has several sub-tables, known as *view*s in SDSS: PHOTOOBJ, which includes all primary and secondary objects; PHOTOPRIMARY, which includes all the primary detections or ones classified as the best version of the objects; PHOTOSECONDARY, which includes the duplicate detection(s); and PHOTOFAMILY, which includes the original undeblended source as well as the sources for which the deblending failed. Based on the morphology, the PHOTOPRIMARY is further divided into STAR (point sources), GALAXY (extended sources), SKY (sky samples), and UNKNOWN (unclassified sources). A PHOTOPRIMARY object is classified as a point source and included in STAR when a PSF fit provides a good approximation to its light profile; otherwise, it is classified as an extended source[8].

As the table with all the unique point source objects, STAR is the repository used by all stellar studies that use the SDSS survey (e.g., Covey et al. 2007; Jurić et al. 2008; Bochanski et al. 2010) including this study. Therefore, it is troublesome that we detected no resolved companions within $1''$ in our search. Given the scope of STAR, it is of utmost importance to understand its completeness level. In particular, it is necessary to quantify the sources that were detected in SDSS but are missing from STAR, i.e., the sources that were misclassified. This would allow any individual study to apply relevant corrections for the sources that were truly missing from SDSS survey (e.g., faintness limit, unresolved binarity).

To test the completeness of STAR, a sample of bona fide stellar sources needs to be used. Fortunately, there exist large spectroscopic samples of confirmed stellar sources in the

[7] http://www.sdss3.org/dr9/algorithms/

[8] More specifically, a point source has PSFMAG − CMODELMAG ≤ 0.145, where PSFMAG and CMODEL are the magnitudes measured by fitting a PSF model and a linear combination of de Vaucouleurs and exponential models, respectively, for an object's light profile.

SDSS catalog. We chose the DR7 catalog of 70,841 M dwarfs from the SDSS West et al. (2011). Each spectrum in this catalog was inspected by eye and verified to be a bona fide M dwarf with relatively high signal-to-noise. Therefore, looking at how these bona fide M dwarfs are cataloged in STAR using only photometric information and how they are flagged should help us understand why we were unable to find binaries tighter than $1''$. As the selection algorithm for M dwarfs in the SDSS spectroscopic survey was not based off STAR (West et al. 2011), this is an ideal sample to investigate how many of the 70,841 bona fide M dwarfs are not included in STAR.

3.1.1. *What is the completeness of DR7 M dwarf sample?*

We performed a PLATE/MJD/FIBERID-based search for the 70,841 M dwarfs in DR7 STAR using the SDSS CasJobs portal and recovered only 66,001 (∼93.2%). When the same search was performed on DR7 PHOTOOBJ, every single spectroscopic target had an counterpart [9]. Appropriate flag cuts (see Section 2) were used in both searches; when excellent photometry was not present, we assumed the sources were not real. That every single M dwarf was in PHOTOOBJ but ∼7% were missing in STAR made it evident that they had been misclassified.

The first type of misclassification (544 instances; ∼0.77% of all sources) happened when an M dwarf was imaged two or more times, and the PRIMARY detection failed the photometric flag cuts but one or more SECONDARY detection(s) passed them. About one-third of the SDSS footprint was imaged multiple times, mostly when plates overlapped each other. In such cases the PRIMARY / SECONDARY classification is based on whether the field was designated as the "primary" field for that area of the sky. As the quality of photometry plays no part in this classification, this is understandable. In fact, it is remarkable that only 0.77% of sources are lost; this incompleteness is largely negligible.

The second kind of misclassification, which happened in 4,295 instances, happened when the M dwarfs were classified as extended sources. This was either because of an nearby extended source contaminated and extended the light profile of the M dwarf or there were two partially resolved stellar sources. (The latter are exactly the kind of sources we are looking for in our binary search.) That ∼6% of all stars could be not cataloged in STAR is rather alarming. We note that this effect is likely exaggerated for the spectroscopic sample (as compared to the entire photometric sample) as a large number of M dwarf spectra were acquired as they were targeted as potential quasars and LRGs (Adelman-McCarthy et al. 2006). Thus, they are more likely to be flagged as being extended sources. However, an incompleteness of ∼6.1% is significant and should be properly accounted for studies that use the SDSS photometric sample.

3.2. *Photometric Distances*

Main-sequence Dwarfs: We determined distances to main-sequence dwarfs using photometric parallax relations that are calibrated from directly-measured trigonometric parallaxes. Even though there is no spectroscopic confirmation, MS dwarfs dominate the stellar sources in the SDSS catalog

[9] This search was done in DR7, from which the spectroscopic catalog was compiled. As each DR is completely new reduction, it is expected that not 100% would be recovered between different DRs. Indeed, we recovered fewer objects when we performed the same search in DR8 and DR9 catalogs.

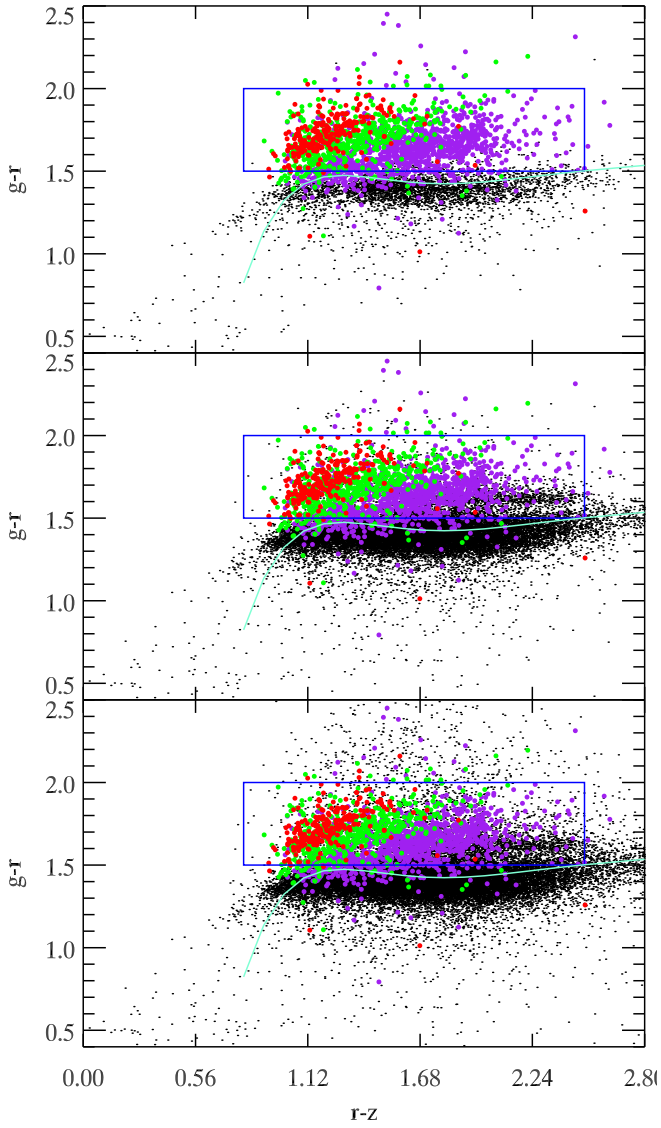

Figure 2. The M subdwarfs, extreme subdwarfs, and ultra subdwarfs (purple, green, and red circles, respectively) are clearly separated from the M dwarfs (black dots). The separation is even cleaner when the photometry is precise; the bottom panel shows all the M dwarfs in SDSS DR7 catalog (West et al. 2011) while the middle and top panels only show ones with uncertainties ≤0.05 and 0.02 mags, respectively. The blue box shows the subdwarf locus identified in Bochanski et al. (2013) for which photometric distances can be calculated.

(Covey et al. 2007). Three separate photometric parallax relations were used, such that the chosen magnitude and colors trace the stellar temperature monotonically in that regime: M_g vs. $g-i$ for F0–K4 (Covey et al. 2007), M_r vs. $r-z$ for K5–M9, (Bochanski et al. 2010), and M_i vs. $i-z$ for L0–L9 (Schmidt et al. 2010) dwarfs. The photometric parallax relations are given in Table 1.

Magnitudes were corrected for extinction, with values from (Schlegel, Finkbeiner, & Davis 1998) as tabulated in the SDSS database, were used in all cases. We adopted an error of 0.3 mag in the calculated absolute magnitudes, which implies a 1σ error of 14% in distance. This scatter is caused by a combination of metallicity, magnetic activity, and unresolved binarity (West et al. 2005; Sesar et al. 2008; Bochanski et al. 2011). The presence of magnetic activity and higher metallicity increases the the intrinsic brightness of a star by

Table 1
Photometric parallax relations used in this paper

type	locus	Photometric parallax relation	References
F0–K4	$-0.01 \leq (r-z) < 0.50$	$M_g = 2.845 + 1.656\ (g-i) + 3.863\ (g-i)^2 - 1.795\ (g-i)^3$	Covey et al. (2007)
K5–M9	$0.50 \leq (r-z) < 4.53$	$M_r = 5.190 + 2.474\ (r-z) + 0.4340\ (r-z)^2 - 0.08600\ (r-z)^3$	Bochanski et al. (2010)
L0–L9	$1.70 \leq (i-z) \leq 3.20$	$M_i = -23.27 + 38.40\ (i-z) - 11.11\ (i-z)^2 + 1.064\ (i-z)^3$	Schmidt et al. (2010)
M subdwarf	$(g-r) > 1.50; 0.8 < r-z < 2.5$	$M_r = 7.9547 + 1.8102\ (r-z) - 0.17347\ (r-z)^2 + 7.7038\ \delta_{g-r} - 1.4170\ (r-z)\ \delta_{g-r}$	Bochanski et al. (2013)
white dwarf	Girven et al. (2011)	iterative fits to DA cooling models	Harris et al. (2006)

as much as a magnitude Bochanski et al. (2011). An unresolved binary companion increases the apparent magnitude by as much as 0.75 mag. Based on high-resolution imaging studies, components of wide binaries are highly likely to harbor close companions (Law et al. 2010). Therefore, we are selecting against triple systems that contain an unresolved binary. However, none of these parameters can be measured or even estimated from the photometry alone. Ivezić et al. (2008) used a photometric metallicity in their photometric parallax relation, but that is applicable only to FGK dwarfs. No such relation is known for M dwarfs, except when they are significantly metal-poor subdwarfs (see below). Therefore, we chose to ignore the metallicity-dependence.

M Subdwarfs: M subdwarfs are low-metallicity, main-sequence dwarfs typically associated with the thick disk or the halo. In the M spectral type, the subdwarfs can be differentiated from the dwarfs by the depleted TiO feature in the optical spectrum (Gizis 1997). In Paper I, we used the reduced proper motions to select subdwarf candidates and identify 70 CPM binaries as subdwarf systems. As a photometric parallax relation had not been calibrated for M subdwarfs, we used the one for M dwarfs. As a result the distances were overestimated and we were able identify only a subset of the subdwarf pairs. Bochanski et al. (2013) have since developed a statistical parallax relation using the SDSS DR7 subdwarf catalog (Savcheva, West, & Bochanski 2014) based on their redder $g-r$ colors. Likely caused by increased hydride absorption, the redder $g-r$ color causes the M subdwarf locus to clearly separate from the M dwarf locus in the $(r-z,\ g-r)$ space (West et al. 2004, 2011; Lépine & Scholz 2008).

Distinguishing the subdwarfs from the dwarfs, however, is not trivial. As shown in Figure 2, while the loci clearly separate in the $(r-z,\ g-r)$ space, the tail of the M dwarf distribution scatters into the subdwarf locus. Given their vastly larger number in the Solar neighborhood, the dwarfs overwhelm the subdwarf population. However, we found that the scatter is in large part due the uncertainty in the magnitude measurements. In Figure 2, the spectroscopically confirmed M dwarfs (West et al. 2011) are plotted as black dots while the spectroscopically confirmed subdwarfs are plotted as purple (subdwarfs), green (extreme subdwarfs), and red (ultra subdwarfs). In the bottom panel, where all the stars plotted, the dwarfs scatter into subdwarf locus (blue box; Bochanski et al. 2013) significantly. However, when only the dwarfs with uncertainties $\leq$0.05 (middle) and $\leq$0.02 mag (top) in the $griz$ bands are plotted, the scatter decreases. While the photometric accuracy for SDSS is $\sim$1% in the $griz$ bands, imposing a 1% or 2% cut seems to exclude a large number of sources. This also biases the sample against fainter and more distant stars like the M subdwarfs. However, when available, exquisite photometry, can be used to select subdwarfs without the need for spectra. This could possibly be extremely beneficial to future photometric surveys like the *Large Synoptic Survey Telescope*.

We chose to accept photometry with uncertainties $\leq$0.05 mag to identify subdwarf candidates. We recognized that this will include some M dwarf interlopers and increase the rate of false positives. However, given the low number of subdwarf binaries known, this is an acceptable risk. We did not include the identified subdwarf systems in the statistical analysis for this paper. We did not include the subdwarf binaries in the analysis for this paper, as they are less likely to be bona fide systems compared to the rest of our sample.

We calculated photometric distances to subdwarf candidates that fit the following criteria:

$$\begin{aligned} g - r &> 1.5 \\ 0.8 < r - z &< 2.5 \\ \mathrm{psfMagErr}_{griz} &<= 0.05 \end{aligned} \quad (1)$$

from the Bochanski et al. (2013) relations. The uncertainty in the absolute magnitude is $\sim$0.41 mag, which translates to a 20% uncertainty in the distance. There were over six million subdwarf candidates, as defined by Eq. 1, in the SDSS photometric catalog.

White Dwarfs: In Paper I we used proper motions to calculate the reduced proper motions and identify potential WD candidates and search for WD companions to the low-mass star sample. Based on $ugriz$ photometry alone, there is no conclusive way to identify potential WD companions around our low-mass dwarf sample. However, in the color–color diagrams, WDs segregate from the main-sequence stars and the quasars. In particular, Girven et al. (2011) have defined a $(g-r,\ u-g)$ locus for hydrogen-atmosphere WDs (DAs) based on a sample of spectroscopically identified DAs (Eisenstein et al. 2006) in SDSS DR7. The efficiency of the photometric selection for the spectroscopic sample was only $\sim$62.3%, after non-DA WDs including WD+MS pairs ($\sim$8.9%), early-type MS stars and subdwarfs ($\sim$11.3%), and quasars ($\sim$17.2%) were removed. However, as quasars were specifically targeted for the SDSS spectroscopic sample, they are disproportionately represented. In the larger photometric sample, the contamination due to quasars is likely to be minor (Girven et al. 2011). Therefore, we use the Girven et al. (2011) $(g-r,\ u-g)$ locus to identify potential WDs but note that >20% of the WD candidates will be interlopers and will require spectroscopic confirmation.

We calculated the photometric distances to candidate DAs by fitting the $ugriz$ photometry to WD cooling models (Bergeron et al. 1995), as specified in Harris et al. (2006). This algorithm fits the photometry to the model in an iterative manner to derive a bolometric luminosity and a distance. However, the composition and mass/gravity is degenerate when only the photometry is available and cannot be determined. So we used the models with pure hydrogen atmospheres and a

gravity of $\log\ g = 8.0$. As our adopted $(g-r, u-g)$ locus selected only DAs, the composition should introduce significant uncertainties in the distances. However, incorrect distances will be derived for WDs with unusually high mass/gravity ($\sim$15% of all WDs), unusually low mass/gravity ($\sim$10% of all WDs), or helium-dominated atmospheres (Harris et al. 2006).

A comparison of our photometric distances and the spectroscopic distances for the DA WDs in the SDSS DR7 catalog (Kleinman et al. 2013) showed a 14–20% scatter (J. Andrews, *private communication*). To be conservative in our matching process, we adopted 14% as the error in our photometric distances. There were 56,505 WD candidates, as selected using the Girven et al. (2011) $(g-r,\ u-g)$ locus, in the SDSS photometric catalog.

3.3. *Binary Candidate Selection*

We searched for stellar sources that had been classified as PRIMARY detections within angular separations of 1–20″ of our sample of 24,036,982 low-mass stars. The inner search radius of 1″ was determined by the SDSS database, as discussed in Section 3.1. We chose the outer search radius to be 20″, after which the number of chance alignments for pairs without proper motions were significant in Paper I (see Figure 1). The search was conducted using in the NEIGHBORS table in the SDSS CasJobs Query interface. Photometric quality cuts, as described above, were performed. We then matched the photometric distances (d) to within 1σ. However, as the error in the distances is a percentage error, we also required the difference in the distance to be less than 100 pc to be classified as a candidate binary pair. Thus, our binary candidate pairs matched the following criteria:

$$\begin{aligned} \theta &= 1 - 20'' \\ \Delta\, d &\leq \min(1\sigma_{\Delta\ d}, 100\ \mathrm{pc}) \\ d &\leq 2500\ \mathrm{pc} \\ |b| &\geq 20^{\circ}. \end{aligned} \tag{2}$$

All stars were selected to have good photometry and PSFMAGERR ≤ 0.10 mag for the bands that are used in their selection and analysis. We identified 514,424 dM+MS, 1212 sdM+sdM, and 642 WD+dM candidate pairs.

3.4. *The Galactic Model: Assessing False Positives in the Binary Candidate Sample*

Despite the rigorous nature of our candidate selection, chance alignments will be present in a sample of wide visual binaries. Such chance alignments arise from the measurement uncertainties in the parameters used in the selection criteria, as well as via the the inherent spreads in these parameters in the Galaxy (Paper I). The number of chance alignments grows as a function of the angular separation ($\propto \theta^2$) and distance. As our search does not include any kinematic matching, the probability of chance alignment is particularly high and, therefore, needs to be rigorously assessed for each and every candidate binary pair. Such a quantitative assessment sifts out false positives from the sample. In Paper I we built a Monte Carlo-based Galactic model that recreated the stellar populations along the line-of-sight (LOS) of a candidate binary and calculated the probability of chance alignments. Based on empirically-measured parameters for the Milky Way, the model accounted for the variations in the stellar number density and space velocities, which become important beyond the Solar Neighborhood. We employed the same model to assess the probability of chance alignment for the binary candidates identified here. The model was described in detail in Paper I; here we only provide a brief synopsis.

Table 2
Galactic Structure Parameters

Component	Parameter name	Parameter description	Adopted Value
	$\rho\ (R_{\odot}, 0)$	stellar density	0.0064
thin disk	$f_{\rm thin}$	fraction[a]	1-$f_{\rm thick}$-$f_{\rm halo}$
	$H_{\rm thin}$	scale height	260 pc
	$L_{\rm thin}$	scale length	2500 pc
thick disk	$f_{\rm thick}$	fraction[a]	9%
	$H_{\rm thick}$	scale height	900 pc
	$L_{\rm thick}$	scale length	3500 pc
halo	$f_{\rm halo}$	fraction[a]	0.25%
	$r_{\rm halo}$	density gradient	2.77
	$q\ (= c/a)$[b]	flattening parameter	0.64

Note. — The parameters were measured using M dwarfs for the disk (Bochanski et al. 2010) and main-sequence turn-off stars for the halo (Jurić et al. 2008) in the SDSS footprint.

[a] Evaluated in the solar neighborhood

[b] Assuming a bi-axial ellipsoid with axes *a* and *c*

Instead of the computationally implausible task of simulating the entire Galaxy with $\gtrsim 10^{11}$ stars, we recreated a $30'' \times 30''$ cone centered at the (α, δ) of each primary out to a distance of 2500 pc. First, we calculated the total number of stars in the conical volume by integrating stellar number density profiles that assume a bimodal disk (Bochanski et al. 2010) and an ellipsoidal halo (Jurić et al. 2008). The model parameters are given in Table 2. While a two-component model is an oversimplification of the complicated scale height distribution (Bovy, Rix, & Hogg 2012), it is easy to model and suffices for our purpose of recreating a random Galaxy. Each LOS was then repopulated with stars using the rejection method (Press et al. 1992). The rejection method ensured that the stars were randomly redistributed while following the overlying stellar number density distribution function. Each star that is generated has a α, δ, and distance[10]. The total number of stars in an LOS ranged between 2000–10000, enough to both produce small-scale density variations as are seen in the Milky Way and perform calculations with relative ease. However, as the number density profiles are smoothed functions that were made to fit to the Galactic field, our model does not produce larger density variations like moving groups, open clusters, or streams.

With the simulated galaxy, we then counted how many stars were found in the ellipsoid that is centered at the α and δ of the binary candidate and defined by its angular separation and its distance errors. This was the same criteria that we used in the search for candidate systems in the SDSS data. Indeed, to conduct the exact same search, we chose to not convolve the luminosity or mass function into the model and rather searched for all stars. As all stars in our simulation are single stars, any star that satisfied the search criteria is a chance alignment. Therefore, the average number of chance alignments is an assessment of the probability that our candidate binary is a false positive. For each candidate pair, we ran 1000 Monte Carlo realizations. If the probability of chance alignment, $P_f \leq 0.10$, we ran a further 4000 realizations for better resolution.

[10] In Paper I we modeled the 3D velocities for each star, but we do not do so here as we are not utilizing proper motions

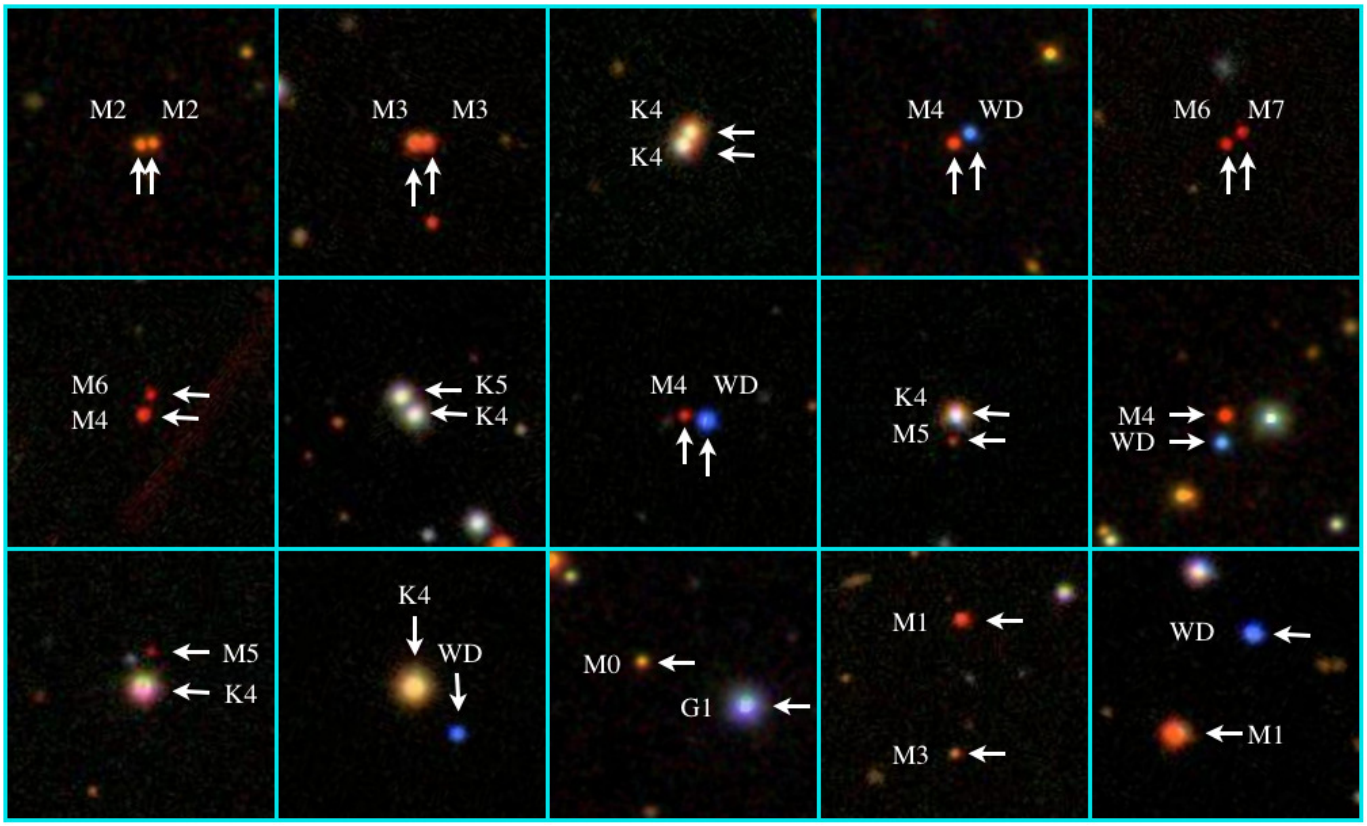

Figure 3. A gri composite collage of SLoWPoKES-II binaries, 48″ on a side. We have identified 105,537 *bona fide* binaries, with at least one component later than K5, without using proper motions.

4. RESULTS: THE SLoWPoKES-II BINARY SAMPLE

Following Paper I we classified candidate pairs with a probability of chance alignment, $P_f \leq 0.05$ as real binaries. We note that this limit does not have any physical motivation but was chosen to minimize the number of spurious pairs. This cut results in 105,537 dM+MS, 450 WD+dM, and 944 sdM+sdM binary systems with separations of 1–20″. 141 of dM+MS binaries are VLM binary candidates Table 4, with $i - z$ colors redder than the median M7 dwarf for both components. Despite the lack of kinematic information, we dub this catalog SLoWPoKES-II. The data for the pairs are tabulated in and is also available in an online visualization portal[5].

This represents a significant increase over the SLoWPoKES catalog of 1342 CPM binaries we presented in Paper I. Each binary has a low probability of chance alignment, with the threshold set at $P_f < 5\%$. Using that threshold, we might expect 5277 of the pairs to be false positives. However, each binary has its own probability of chance alignment, based on the size of the binary and its position in the Galaxy, that in most cases is significantly lower than 5%. Based on those probabilities, we expect only 2464 (or 2.33%) of the binaries to be false positives.

Figure 3 shows a collage of gri composite images, 48″ on a side, of 15 SLoWPoKES-II binaries. The inferred spectral types of MS dwarfs, based on their $r - z$ colors, are shown for each component. Table 3 summarizes the SLoWPoKES-II catalog, with the properties of the systems and positions and photometry of both components included. Table 4, Table 5, and Table 6 summarize the candidate VLM, WD+dM, sdM+sdM systems, respectively. While these systems are also analyzed with the Galactic model and required to have $P_f < 5\%$, their classification as an sdM, VLM, or WD is based on photometry alone. This adds a level of uncertainty that the Galactic model cannot quantify. For that reason, these samples are likely to be contaminated at a higher rate than the SLoWPoKES-II sample in Table 3. Thus, we do not include samples in the analysis presented in this paper.

Both the SLoWPoKES and SLoWPoKES-II catalogs are publicly available on the worldwide web[5] via the Filtergraph portal (Burger et al. 2013). We hope this will enable to the entire community to interact with and visualize this large data set using a dynamic, multi-dimensional plotting applet. The table view Filtergraph is also an easy medium to select targets for followup observations.

4.1. *Identifying bona fide wide binaries without kinematics*

Figure 4 shows the number density of the 514,424 binary candidates, identified in Section 3.3, as a function of the probability of chance alignment, P_f, and angular separation. As would be expected, the number of candidate pairs grows sharply with angular separation. There is also a large spread in P_f at a given separation, reflecting the varying stellar densities along different lines-of-sight. Especially at the large angular separations, the P_f is quite high for a large number of candidates, indicating that they are chance alignments. Therefore, we applied the $P_f \leq 5\%$ cut, shown as the red line, for the candidates to be included in the SLoWPoKES-II catalog. This is a fairly conservative cut but serves to minimize the number of false positives. It is also the same threshold that we used in Paper I, although the SLoWPoKES systems had proper motions and, hence, should have a much lower rate of false positives. The middle panel shows the histogram of fraction of candidate binaries that passed this threshold as a function of

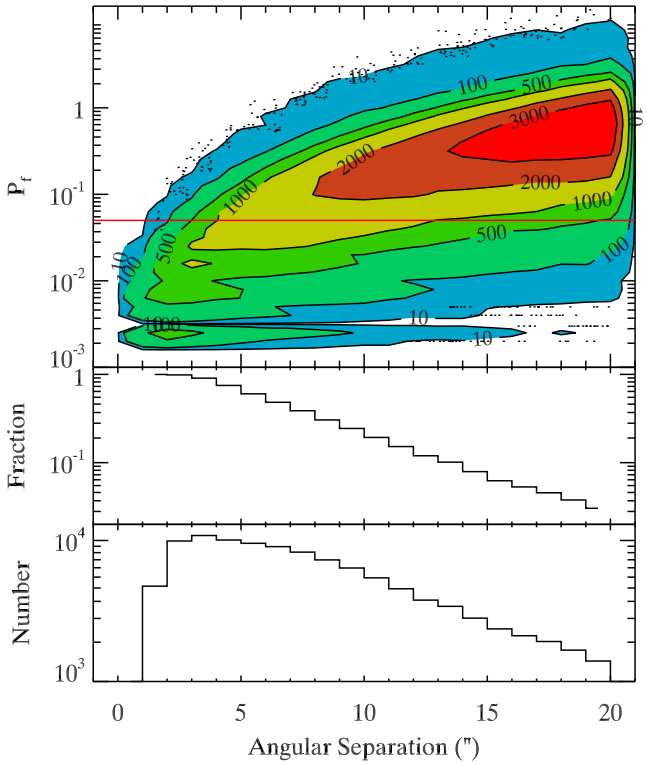

Figure 4. The number density, as represented by the contours, of the 514,424 binary candidates as a function of P_f as calculated by the model vs. the angular separation and distance. The red line is the threshold P_f that we adopted for the SLoWPoKES-II catalog. The fraction of candidates that passed the P_f threshold—which quantifies the number of chance alignments expected within the bounds of that particular binary—are shown in the middle panels while the distribution of the resultant 105,537 SLoWPoKES-II binaries are shown in the bottom panels.

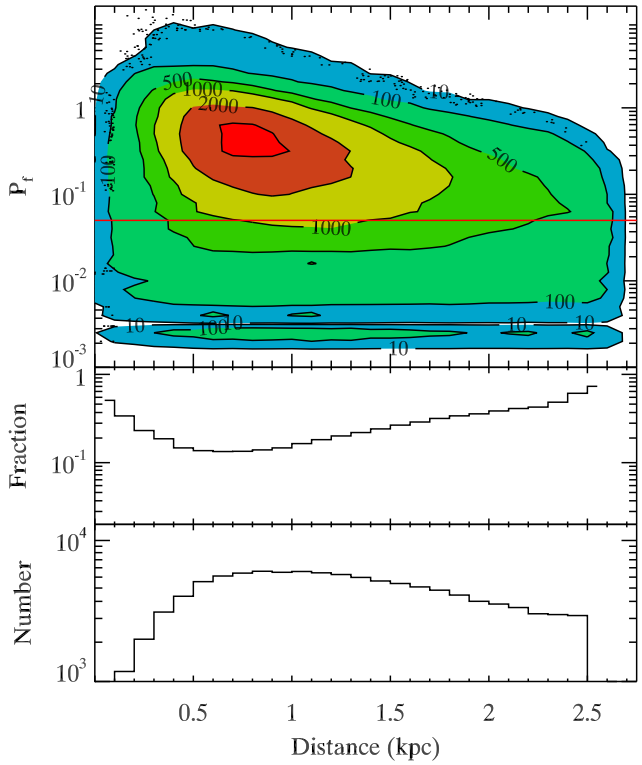

Figure 6. The number density, as represented by the count-ours, of the 514,424 binary candidates as a function of P_f and distance. The red line is the threshold P_f that we adopted for the SLoWPoKES-II catalog. The fraction of candidates that passed the P_f threshold are shown in the middle panels while the distribution of the resultant 105,537 SLoWPoKES-II binaries are shown in the bottom panels.

angular separation. All of the candidate pairs within 3″ but only ∼2% of the pairs at 20″ were vetted to be real binaries by the Galactic model. The bottom panel shows the angular separation histogram for the 105,537 binaries in SLoWPoKES-II catalog. This distribution is strongly skewed towards smaller separations, with 51% of the pairs at 1″–7″ and 72% at 1″–10″.

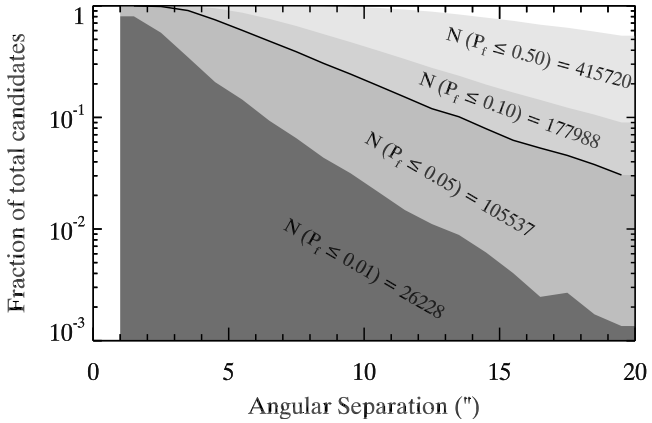

Figure 5. The fraction of binary candidates that meet the $P_f \leq 1\%$, 5%, 10%, and 50% thresholds as a function of angular separation. The number of pairs that meet each threshold is also shown. We have chosen $P_f \leq 5\%$ (dark line) for the SLoWPoKES-II catalog, resulting in 105,537 wide binaries.

Figure 5 shows the distribution of the fraction of binary candidates that pass various P_f thresholds: ≤ 1%, 5%, 10%, and 50%, with the total number of candidates also shown. Obviously, as we discussed in Paper I, the choice of a threshold is subjective and depends on the need. For example, if a followup study needed to minimize the number of false positives, a sample with $P_f \leq 1\%$ should be chosen. However, if the study needed bright, rare binaries (e.g., WD+dM binaries), it might need to tolerate the high number of false positives and select candidates with $P_f \leq 10\%$. With such a large number of binary candidates, there is a flexibility in the number and types of binary systems that is available to followup studies.

Figure 6 shows the number density of all candidate pairs as a function of P_f and photometric distance. In general, P_f is flat as a function of the distance, indicating that the distance of a given pair has no significant effect on how likely it is to be a chance alignment. More significantly, the number of candidate pairs peaks around ∼800 pc and declines smoothly afterwards. This is because an additional selection criteria, $\Delta\, d \leq 100$ pc (Eq. 2), which becomes effective at large distances and rejects pairs with $\Delta\, d$ within 1 $\sigma_{\Delta d}$ but larger than 100 pc. So even as the search volume grows larger, the number of candidates actually decreases. However, the resulting candidates are more likely to be binaries, as shown in the middle panel: the fraction of candidate binaries that pass the $P_f \leq 5\%$ threshold reaches a minimum at ∼700 pc and increases sharply afterwards. In fact, the acceptance rate for binaries at ∼2200–2500 pc is higher than for binaries at any other distance. At these distances, $\Delta\, d \leq 100$ pc implies that the distances match within 6–7% of each other, explaining the low rate of false positives. Therefore, as shown in the lower panel

of Figure 6, there are a relatively large number of identified binaries at large distances.

4.2. *Distribution of binary separations*

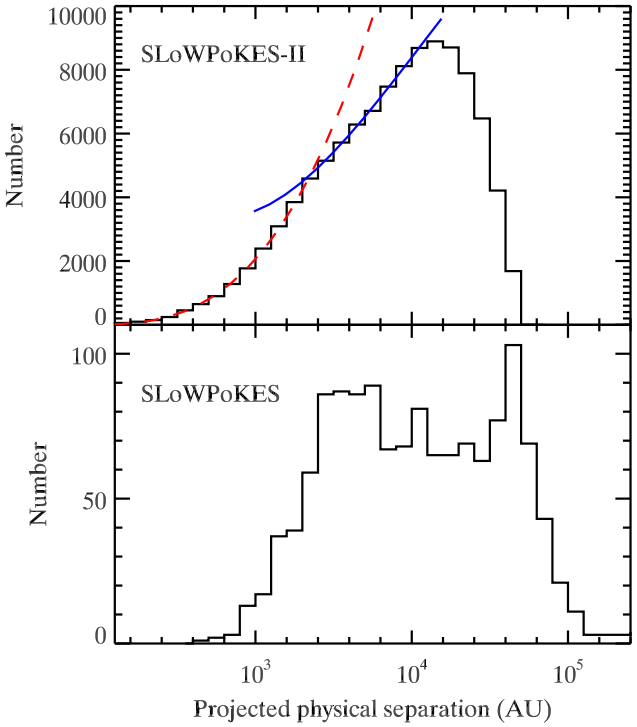

Figure 7. The distribution of projected physical separations for the SLoWPoKES-II binaries (top) and the SLoWPoKES CPM binaries (bottom). As SLoWPoKES-II was restricted to $\theta \lesssim 20''$, it only probes binaries smaller than ∼50,000 AU, thus missing the widest systems. Even so, the slowpokes-II distribution cannot be fit by a single functional form. We fit two polynomials with a break at $a = 10^{3.4}$ AU, shown in dashed red and solid blue lines in the figure. This inflection point suggests the presence of multiple populations of wide binaries.

Figure 7 shows the distribution of projected physical separations of the SLoWPoKES and SLoWPoKES-II binaries.[11] The SLoWPoKES distribution exhibited a bimodal distribution, which we interpreted as either the presence of two formation modes or the preferential destruction of the widest pairs in the timescale of a 1–2 Gyr (Paper I). These binaries were 7–180″ systems, within an average distance of 1000 pc. In SLoWPoKES-II, we are not sensitive to binaries as wide, as the lack of proper motions limits us to angular separations of 1–20″; however, the binaries are up to 2500 pc away. Clearly, the selection biases and the resultant distributions of the identified binaries involved are markedly different. For example, the steep falloff of the SLoWPoKES-II distribution at $a > 10^{4.1}$ AU is due to our insensitivity to binaries at those separations.

[11] In Paper I we used a statistical correction to scale the projected physical separation to semi-major axis; however, Dupuy & Liu (2011) have shown that the correction factor is significantly smaller and highly dependent on the orbital parameters. They calculated correction factors based for their sample of <4 AU binaries. The sample presented here are in a completely different separation regime, making it unlikely that the same correction factors can be used. Therefore, we have eschewed semi-major axis and chosen to work in projected physical separation space.

In Paper I we found a dip in the distribution of binary separations at $a \sim 10^4$ AU (bottom panel of Figure 7), but at first glance this is not apparent in the new SLoWPoKES-II distribution (top panel). However, there is an inflection point at $a \sim 10^{3.4}$ AU (2500 AU), where the slope of the distribution becomes noticeably shallower. In Figure 7, two power-law fits are shown on either side of the inflection at $a \sim 10^{3.4}$ AU. This inflection is at a similar separation scale as seen in previous samples of binary stars (Allen et al. 2000; Lépine & Bongiorno 2007), which were interpreted as wider binaries being disrupted beyond a critical separation and being less common, as was originally predicted by Öpik (1924). However, it is much smaller than the bimodality seen in Paper I at ∼20,000 AU. Whether present at formation or sculpted later in life, the multiple modes in binary populations is intriguing and suggests that interstellar interactions are more common than thought.

4.3. *Binary mass distribution*

Figure 8 shows the $g - i$ and $r - z$ color distributions for the primary (left) and secondary (right) components of the SLoWPoKES-II binaries. The primary is defined as the component with the bluer $r - z$ color. The histograms for the color distributions are shown along the top and sides of each panel. The inferred spectral types, based on the median color–spectral type relations (Covey et al. 2007; West et al. 2011), are shown along the top axes. In general, the SLoWPoKES-II binaries reflect the SDSS low-mass dwarf population in both $g-i$ and $r-z$ colors. The distributions peak between the M2–M4 spectral types, same as the field mass function (Bochanski et al. 2010). The primary color distributions also exhibit a pileup at the bright end of the distribution, which is most likely a selection bias. SLoWPoKES-II binaries span a large range of colors (and masses). There are a significant number of primary components from early–mid G to the mid-M dwarfs while the secondaries extend from K5 to the M9 spectral types. The blue end of the secondary component distributions are defined by the color cuts imposed on our initial target sample ($r - i \geq$0.3, $i - z \geq$ 0.2). While SLoWPoKES contained only a handful of binaries after ∼M6–M7, there are now a significant number of binaries at the low-mass end of the stellar main sequence at large distances.

Figure 9 shows mass ratio distribution of SLoWPoKES-II binaries as a histogram (top) and a cumulative distribution function (bottom). The black line and dots represent the entire catalog while the red, purple, blue, and cyan show distributions for different primary masses. The masses were calculated by interpolating from their $g - i$, $r - z$ colors, or $i - z$ based on Kraus & Hillenbrand (2007a). We set the lowest mass at 0.075 $M_\odot$, the hydrogen burning minimum mass (Burrows et al. 1997), as the $i - z$–mass relation is even less constrained at lower masses. All of the distributions are skewed towards similar masses, with notable deficit at the lowest mass ratios, below q ∼0.4. This is mostly due to an additional selection criterion that at least one component be K5 or late (≤0.70 $M_\odot$), which means the lowest mass ratio possible for a K5 primary is ∼0.11. Moreover, the steep mass–luminosity ratio among the M spectral types means SDSS photometry would only detect a M6 or earlier companion for the K5 primary, restricting the lowest possible mass ratio to ∼0.17. Similarly, for a M4 primary (∼0.20 $M_\odot$), the observed mass ratio is always greater than 0.39. After q ∼0.4, the various cumulative distributions show a relatively smooth progression that is similar for the different masses. There is a

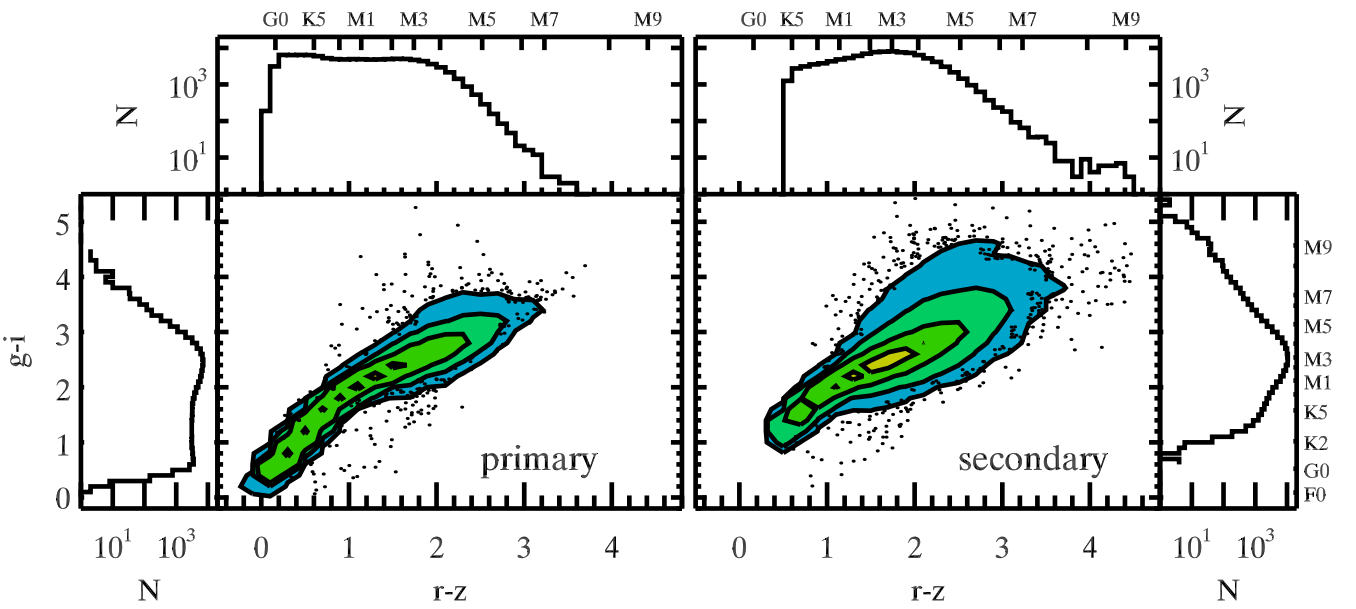

Figure 8. The $g-i$ and $r-z$ color distributions for the primary (left) and secondary (right) components of the SLoWPoKES-II binaries, with the contour levels at 10, 100, 1000, and 5000. The histograms of the distributions are plotted along the sides, and the inferred spectral types are also shown. We defined the primary component to be have the bluer $r-z$ color. Both the primary and the secondary distributions show definitive peaks at ∼M2–M4 spectral types in both the $g-i$ and $r-z$ colors. As our initial target sample used a cutoff on the $r-i$ and $i-z$ colors at ∼K5 spectral type, there is a sharp cutoff at the blue end of the $r-z$ distribution for the secondary component.

preference for a larger q at the lowest masses and a smaller q at the highest masses, but those are most likely due to selection biases as discussed above.

5. DISCUSSION

We have assembled a large sample of 105,537 wide binaries with projected physical separations of ∼1000–60,000 AU. The identification was based on matching 3D position of stars in the SDSS photometric sample and assessing the probability of chance alignment with our Galactic model. All of the binaries in the SLoWPoKES-II catalog have a probability of chance alignment of $\lesssim$5%. For comparison, the original SLoWPoKES contained 1342 CPM binaries with separations of 7″–180″ (500–100,000 AU) at ∼100–800 pc. While our initial aim was to combine these two samples for a detailed analysis, the regimes they probed are much different. For example, despite extending to $\gtrsim$2000 pc, the widest SLoWPoKES-II binary is a factor of two smaller than the widest SLoWPoKES binary. Proper motions allowed for the identification of CPM binaries up to 180″, whereas we were restricted to 20″ in this paper. Thus, even though the two samples are are neither complete nor continuous, they are complementary and are both of high fidelity.

5.1. *SLoWPoKES-II: A rich, diverse catalog of binaries*

In addition to being the largest catalog of wide binaries, SLoWPoKES-II contains a diversity of systems—in mass, mass ratios, metallicity, separations, evolutionary states, and Galactic positions—that should facilitate followup studies to characterize the properties of low mass stars. In addition, we have identified three specific subsets of candidate binaries that are rare: (i) wide VLM systems, (ii) WD+dM systems, and (iii) sdM+sdM binaries. They could prove uniquely useful in characterizing those stellar types.

The diversity of systems should allow for in-depth probes of different aspects of low-mass stellar physics. Specifically, the flexibility offered by the large sample size and all-sky nature of SLoWPoKES-II could be exploited by large spectroscopic surveys where fibers are often available in certain parts of the sky. For example, we were awarded 1000 fibers in the Baryon Oscillation Spectroscopic Survey of SDSS-III (BOSS; Dawson et al. 2013) to acquire spectra of 500 SLoWPoKES-II binaries. This was in addition to the 1000 fibers awarded earlier for the SLoWPoKES binaries. We are using the combined sample ∼1000 binaries to ascertain the age–activity and metallicity relationships in low-mass M dwarfs (Massey et al. *in prep.*).

5.2. *Multiple pathways for wide binary formation*

In Paper I we noted the presence of a bimodality in the physical separation distribution of the binaries (Figure 7). When compared to the dynamical dissolution timescales (Weinberg et al. 1987), the bimodality in the SLoWPoKES distribution led us to suggest that it comprised of two different population of binaries with a break at ∼20,000 AU: (1) a "wide" population that is dynamically stable over ∼10 Gyr and (2) an "ultra-wide" population of young, loosely-bound systems that will dissipate in 1–2 Gyr. In a followup high-resolution imaging study with the Keck II and Palomar Laser Guide Systems with Adaptive Optics, we found that the frequency of a close companion was higher in wide binaries than in single stars (Law et al. 2010). Moreover, the frequency increased significantly with wide binary separation, suggesting that different formation modes were at work.

In SLoWPoKES-II we have found further evidence of multiple populations in the distribution of physical separations (Figure 7). While more subtle than in Paper I, a break is clearly evident at ∼2500 AU. This is much smaller than the critical separation in Paper I but approximately where we saw the first peak in the SLoWPoKES sample. It is also at the same separation scale as seen in previous studies (Öpik 1924; Allen et al. 2000; Lépine & Bongiorno 2007). That an inflection in the separation distribution stands out amongst the myriad of selection biases and incompletenesses is quite sig-

nificant. Further investigation into these multiple populations and their origins is clearly warranted. Whether wide binary distributions are segregated at birth (e.g., Reipurth & Mikkola 2012) or sculpted as they traverse around the Milky Way (e.g., Weinberg et al. 1987; Jiang & Tremaine 2010) has important implications on our interpretation of observed binary populations and, consequently, on our understanding of binary star formation.

There are no signatures of multiple populations in the color (a proxy for mass; Figure 8) or mass ratio (Figure 9) distributions. Even if there were such signatures were present, identifying them from amongst the selection biases without further data would be extremely difficult. Recently, there has been extensive discussion on the formation and stability of the extremely wide systems. This has partly been motivated by the large samples of wide binaries that have become available over the past decade (e.g., Chanamé & Gould 2004; Lépine & Bongiorno 2007; Sesar et al. 2008; Dhital et al. 2010). In addition, such wide binaries have been identified at very young ages in Orion (Connelley, Reipurth, & Tokunaga 2009) and in Taurus and Upper Sco (Kraus & Hillenbrand 2009b). Numerical simulations have explored mechanism that would form wide binaries primordially or via dynamical interactions, with three different pathways suggested. First, observations of protostars at the end of long, extended filaments of molecular gas (Tobin et al. 2010) argues that wide binaries can form with primordial separations of ∼0.1 pc. Second, primordial triple or quadruple systems become extremely hierarchical by scattering or even ejecting one of the components (Reipurth & Mikkola 2012). Third, simulations have shown wide binaries forming in the halo of clusters via dynamical interactions or as they escape the cluster (Bate & Bonnell 2005; Kouwenhoven et al. 2010; Moeckel & Bate 2010; Moeckel & Clarke 2011). These pathways are unique and expected to imprint distinct signatures on the resultant population. For example, the Reipurth & Mikkola (2012) pathway would produce a high frequency of triples and quadruples while dynamical interactions would produce a very high proportion of low-mass binaries.

There is no clear evidence from the SLoWPoKES samples that any of these pathways are dominant. Rather, there is reason to believe all of the pathways could be operational. Without a reliable age indicator there is no way to observationally determine if components of an wide binary formed together. In fact, it might be impossible to do so even with an age indicator as the age difference of a few million years can be indistinguishable once the stars are in the Galactic field. We suggest that there is no principal pathway for wide binary formation. Determining the relative efficiencies of the different formation modes would be more valuable.

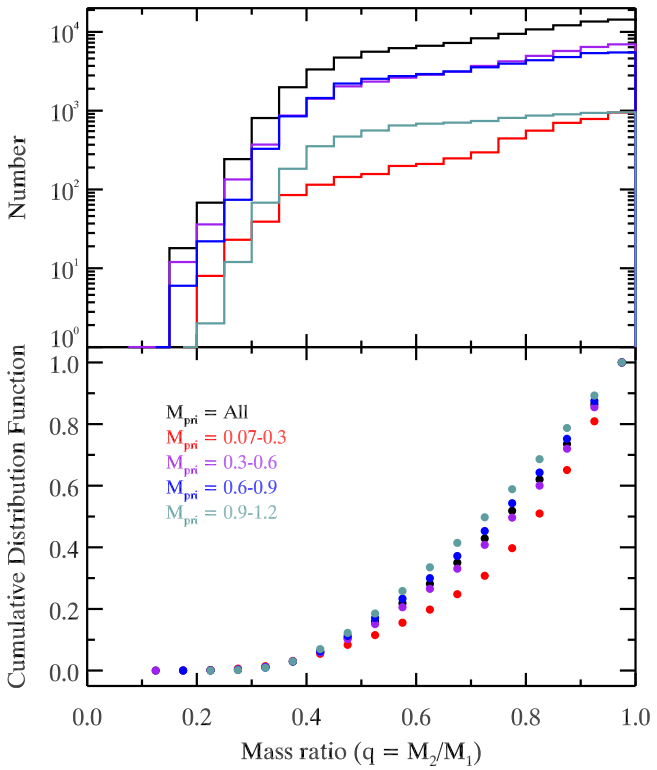

Figure 9. The mass ratio distribution of SLoWPoKES-II systems shown as histogram (top) and a cumulative distribution function (bottom). The black line and dots show the all the SLoWPoKES-II binaries while the red, purple, blue, and cyan show the distributions for systems with different primary masses. masses were calculated by interpolating from their $g-i$ and $r-z$ colors using Kraus & Hillenbrand (2007a); the minimum mass was set at 0.075 $M_\odot$. There is a large bias towards systems with similar masses, with the median mass ratio being ∼0.78. While the systems with larger primary masses seem more likely to have low mass ratios as compared to systems with low-mass primary, it is largely due to biases inherent in SDSS and our identification techniques.

5.3. *Wide VLM binaries: Too numerous for the ejection hypothesis?*

SLoWPoKES did not contain wide very low-mass (VLM; M $\lesssim$ 0.1 $M_\odot$ Burgasser 2007) or brown dwarf (BD) binaries. They were too red and too faint to be detected in the USNO-B survey and, therefore, did not have measured proper motions. Finding more VLM/BD systems was one of our primary motivations for identifying binaries without proper motions. Only eleven wide ($\gtrsim$100 AU) VLM/BD systems are currently known, including a VLM triple at 820 AU (Burgasser et al. 2012) and binaries at 5100 AU (Artigau et al. 2007) and 6700 AU (Radigan et al. 2009). With the formation processes and techniques to measure properties for VLM/BDs not completely understood, the value of a larger sample could not be overstated.

Until recently, the processes by which very low mass (VLM; M $\lesssim$ 0.1 $M_\odot$ Burgasser 2007) stars and brown dwarfs (BDs) form were thought to be different from those of higher-mass stars. Reipurth & Clarke (2001) suggested that VLM/BDs are protostars that are ejected from their natal cores before they can accrete and grow to stellar masses. Such ejections were seen in numerical simulations (e.g., Bate et al. 2002), and all observed VLM/BD binaries had enough binding energy to have survived such ejections (Burgasser et al. 2003; Close et al. 2003). However, with the discovery of each subsequent VLM/BD binary wider than ∼100 AU, the viability of the ejection hypothesis had been called into question (e.g., Dhital et al. 2011; Burgasser et al. 2012).

Figure 10 shows the projected physical separation distribution for a sample of 141 binaries with $i-z \geq 1.14$, the median color of an M8 dwarf (West et al. 2011). While spectroscopic followup are ongoing to confirm their spectral types (a proxy for mass), it seems clear that significant number of systems with separations of 1000–5000 AU exist in the Galactic field. We note that photometric colors can be particularly deceiving in the VLM/BD regime, so the need for spectra cannot be overemphasized. However, such a large number of in wide VLM binary candidates can inform us a lot about their forma-

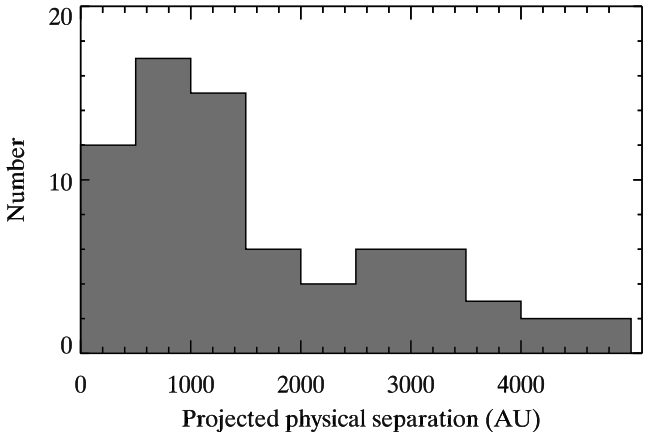

Figure 10. Distribution of SLoWPoKES-II wide binaries, at the end of the main sequence. These were selected by requiring $i - z \geq 1.14$, the median color for a M8 dwarf (West et al. 2011). As only eleven wide VLM binaries are currently known, a larger population has strong implications on how we interpret star formation at the lowest masses.

tion. [12] These systems most definitely did not form primordially via ejection, as their binding energy is too small to have survived a dynamical kick. With 11 previous systems and 141 candidates presented here, we cannot explain away the wide VLM binary population as exceptions.

The alternative pathway to VLM/BD formation is that they form in a manner similar to stars via gravoturbulent fragmentation (Hennebelle & Chabrier 2011; Jumper & Fisher 2013). The detection of the first pre-BD core, *Oph B-11* (André et al. 2012), has helped further that idea significantly. Our sample does not allow for rigorous testing of this hypothesis; we will wait for followup observation that will better characterize the binaries. However, neither the separation distribution nor the mass ratio distribution show any significant change as a function of mass. While the systems with less massive primaries are more likely to be equal-mass (Figure 9). This characteristic is a bias of our sample mostly due to insensitivity to lower-mass, fainter companions and to setting the minimum mass at 0.075 $M_{\odot}$. The trend of more equal-mass binaries is also a gradual change at all masses, with no significant break at the VLM/BD regime.

There is no suggestion of multiple populations of wide VLM binaries, as was observed for wide stellar binaries in Section 5.2. However, we cannot discount the possibility that these wide VLM binaries were bound post-formation (Kouwenhoven et al. 2010; Moeckel & Bate 2010; Moeckel & Clarke 2011). Numerical simulations show that a molecular core typically fragments into 3–5 cores, whence the smaller cores are ejected before they can grow into stellar masses (Bate 2012). Open clusters could have hundreds of these VLM protostars floating around, increasing the likelihood of multiple ones interacting at the same time and forming wide, gravitationally-bound systems. The efficiency of these capture-like processes could be much higher in the VLM/BD regime.

6. CONCLUSION

We have identified the SLoWPoKES-II catalog of 105,537 wide, low-mass binaries without using proper motions. While false positives are inherent in all statistical samples, we have required a relatively stringent probability of chance alignment, P_f, as calculated by our Galactic model to be $\leq$5% for each of our binaries. Most binaries have a much smaller probability of chance alignment. The entire sample is expected to have 2464 (2.3%) chance alignments. In addition, we have identified 944 sdM+sdM and 450 WD+dM candidate binaries, which also have a $\leq$5% probability of chance alignment. However, as their identification as an sdM or WD is based on photometry alone, there is a higher probability of them being false positives.

The STAR table in SDSS suffers from a $\sim$6% incompleteness. In particular, $\sim$6% of the spectroscopically confirmed, *bona fide* M dwarfs (West et al. 2011) are missing are not included in STAR. Instead, they are classified as extended sources due to the presence of a nearby or partially resolved stellar object. This incompleteness could be exaggerated for the spectroscopic sample as a significant number of M dwarfs were observed as potential galaxies and quasars (Adelman-McCarthy et al. 2006). We advise caution when using the STAR table, especially for studies that seek to do a complete census or build a complete sample of stars in the Galaxy.

SLoWPoKES-II binaries have projected physical separations of 500–50,000 AU at distances up to 2500 pc. We are not sensitive to binaries as wide as the ones identified in (Paper I) as only searched within 20″. Given the dynamic magnitude limits of the SDSS, our sample is likely largely dominated by a confluence of selection biases making is hard to construct or even complete samples. For example, the color distributions for both the primary and secondary components show a higher proportion of G- and K-type dwarfs, as compared to the field population (Bochanski et al. 2010). This is likely because they are brighter and more likely to have been detected. With complete samples not feasible, the main contribution of SLoWPoKES-II is the large, diverse sample of binaries that will facilitate detailed studies of low-mass star properties. Sub-samples are already part of various studies to probe the age–activity, rotation–age, and metallicity of M dwarfs. Most importantly, SLoWPoKES-II contains a significant number of binaries at the late-M spectral types, enabling the studies to probe into the very bottom of the main sequence.

The distribution of binary physical separations exhibits a marked inflection which can be interpreted as representing two binary populations, consistent with our results in Paper I and Law et al. (2010). While the incompleteness in our sample and lack of any way to quantify or correct for that incompleteness prevents us from characterizing the populations, the separation distribution exhibits a marked inflection which can be fit by two more polynomials. Combined with our results in Paper I and Law et al. (2010), we infer that the wide binary population in the Galactic field is composed of multiple different populations, either from different formation mode or via different dynamical histories.

We have identified 141 wide binaries in which both components are VLMs. This is 7$\times$ larger than the current sample of wide, VLM binaries. While spectroscopic data are needed to confirm their VLM status, it is becoming clear that wide VLM binaries are not exceptions. These wide systems are critical in understanding VLM/BD formation, as their binding energies are too low to have formed via the ejection mechanism (Reipurth & Clarke 2001). As searches go deeper and identify more wide, VLM binaries, it looks unlikely that VLM/BDs are formed primarily via ejection. The data indicate that there is no change in formation mechanism with stellar mass, suggesting VLM/BDs are also formed via gravoturbulent fragmentation, like their more massive counterparts (Hennebelle

[12] For reference, the current sample of all VLM binaries is $\gtrsim$120 (T. Dupuy, *priv. comm.*).

& Chabrier 2011; Jumper & Fisher 2013).

The SLoWPoKES and SLoWPoKES-II catalogs are available on the Filtergraph portal[5]. (Burger et al. 2013). The portal allows for dynamic plotting of these large data sets and real-time filtering of the data using user-specified criteria. It is useful for target selection as its smoothly transitions between graphical and tabular visualizations of the data and allows for selection of data points with the keyboard or the mouse.

Lastly, we have demonstrated a methodology to identify bona fide wide binaries using just photometry together with a galactic model to assess false positives. Really, this technique harks back to Michell (1767)'s discovery of "double" stars, where he argued that some pairs of stars were too close to each other, as compared to mean distances between stars, to be unrelated. We have used the all-sky data from SDSS and our understanding of the Galaxy's stellar distribution to statistically identify bona fide binary stars without the advantage of proper motions.

The authors would like to thank Jeff Andrews, Matthew Bate, Adam Burgasser, Ben Burningham, Rebecca Oppenheimer, and Leigh Smith for useful discussions and Dan Burger for help with setting up the online data visualization portal.

SD, AAW, and KGS acknowledge funding support through NSF grant AST–0909463. AAW also acknowledges support through AST–1109273.

This work was conducted in part using the resources of the Advanced Computing Center for Research and Education at Vanderbilt University, Nashville, TN.

Funding for the SDSS and SDSS-II was provided by the Alfred P. Sloan Foundation, the Participating Institutions, the National Science Foundation, the U.S. Department of Energy, the National Aeronautics and Space Administration, the Japanese Monbukagakusho, the Max Planck Society, and the Higher Education Funding Council for England. The SDSS was managed by the Astrophysical Research Consortium for the Participating Institutions.

We acknowledge use of the ADS bibliographic service.

REFERENCES

Adelman-McCarthy, J. K., Agüeros, M. A., Allam, S. S., et al. 2006, ApJS, 162, 38
Aihara, H., Allende Prieto, C., An, D., et al. 2011, ApJS, 193, 29
Allen, C., Poveda, A., & Herrera, M. A. 2000, A&A, 356, 529
André, P., Ward-Thompson, D., & Greaves, J. 2012, Science, 337, 69
Andrews, J. J., Agüeros, M. A., Belczynski, K., et al. 2012, ApJ, 757, 170
Andrews, J. J., Agüeros, M. A., Gianninas, A., et al. 2015, ApJ, submitted
Artigau, É., Lafrenière, D., Doyon, R., et al. 2007, ApJ, 659, L49
Bate, M. R. 2012, MNRAS, 419, 3115
Bate, M. R., & Bonnell, I. A. 2005, MNRAS, 356, 1201
Bate, M. R., Bonnell, I. A., & Bromm, V. 2002, MNRAS, 332, L65
Bergeron, P., Wesemael, F., & Beauchamp, A. 1995, PASP, 107, 1047
Bochanski, J. J., Hawley, S. L., Covey, K. R., et al. 2010, AJ, 139, 2679
Bochanski, J. J., Hawley, S. L., & West, A. A. 2011, AJ, 141, 98
Bochanski, J. J., Savcheva, A., West, A. A., & Hawley, S. L. 2013, AJ, 145, 40
Bochanski, J. J., West, A. A., Hawley, S. L., & Covey, K. R. 2007, AJ, 133, 531
Bovy, J., Rix, H.-W., & Hogg, D. W. 2012, ApJ, 751, 131
Burgasser, A. J. 2007, ApJ, 659, 655
Burgasser, A. J., Kirkpatrick, J. D., Reid, I. N., et al. 2003, ApJ, 586, 512
Burgasser, A. J., Luk, C., Dhital, S., et al. 2012, ApJ, 757, 110
Burger, D., Stassun, K. G., Pepper, J., et al. 2013, Astronomy and Computing, 2, 40
Burrows, A., Marley, M., Hubbard, W. B., et al. 1997, ApJ, 491, 856
Chanamé, J., & Gould, A. 2004, ApJ, 601, 289
Close, L. M., Siegler, N., Freed, M., & Biller, B. 2003, ApJ, 587, 407
Connelley, M. S., Reipurth, B., & Tokunaga, A. T. 2009, AJ, 138, 1193
Covey, K. R., Ivezić, Ž., Schlegel, D., et al. 2007, AJ, 134, 2398
Cutri, R. M., Skrutskie, M. F., van Dyk, S., et al. 2003, 2MASS All Sky Catalog of Point Sources. (The IRSA 2MASS All-Sky Point Source Catalog, NASA/IPAC Infrared Science Archive. http://irsa.ipac.caltech.edu/applications/Gator/)
Dawson, K. S., Schlegel, D. J., Ahn, C. P., et al. 2013, AJ, 145, 10
Delfosse, X., Beuzit, J.-L., Marchal, L., et al. 2004, in Astronomical Society of the Pacific Conference Series, Vol. 318, Spectroscopically and Spatially Resolving the Components of the Close Binary Stars, ed. R. W. Hilditch, H. Hensberge, & K. Pavlovski, 166–174
Dhital, S., Burgasser, A. J., Looper, D. L., & Stassun, K. G. 2011, AJ, 141, 7
Dhital, S., West, A. A., Stassun, K. G., & Bochanski, J. J. 2010, AJ, 139, 2566
Dhital, S., West, A. A., Stassun, K. G., et al. 2012, AJ, 143, 67
Dupuy, T. J., & Liu, M. C. 2011, ApJ, 733, 122
Eisenstein, D. J., Liebert, J., Harris, H. C., et al. 2006, ApJS, 167, 40
Eisenstein, D. J., Weinberg, D. H., Agol, E., et al. 2011, AJ, 142, 72
Fadely, R., Hogg, D. W., & Willman, B. 2012, ApJ, 760, 15
Fischer, D. A., & Marcy, G. W. 1992, ApJ, 396, 178
Fukugita, M., Ichikawa, T., Gunn, J. E., et al. 1996, AJ, 111, 1748
Girven, J., Gänsicke, B. T., Steeghs, D., & Koester, D. 2011, MNRAS, 417, 1210
Gizis, J. E. 1997, AJ, 113, 806
Gunn, J. E., Carr, M., Rockosi, C., et al. 1998, AJ, 116, 3040
Gunn, J. E., Siegmund, W. A., Mannery, E. J., et al. 2006, AJ, 131, 2332
Gunning, H. C., Schmidt, S. J., Davenport, J. R. A., et al. 2014, PASP, 126, 1081
Harris, H. C., Munn, J. A., Kilic, M., et al. 2006, AJ, 131, 571
Hauschildt, P. H., Allard, F., & Baron, E. 1999, ApJ, 512, 377
Hawley, S. L., Gizis, J. E., & Reid, I. N. 1996, AJ, 112, 2799
Hennebelle, P., & Chabrier, G. 2011, ApJ, 743, L29
Henry, T. J. 1998, in Astronomical Society of the Pacific Conference Series, Vol. 134, Brown Dwarfs and Extrasolar Planets, ed. R. Rebolo, E. L. Martin, & M. R. Zapatero Osorio, 28
Henry, T. J., & McCarthy, D. W. J. 1993, AJ, 106, 773
Ivezić, Ž., Sesar, B., Jurić, M., et al. 2008, ApJ, 684, 287
Jiang, Y., & Tremaine, S. 2010, MNRAS, 401, 977
Jumper, P. H., & Fisher, R. T. 2013, ApJ, 769, 9
Jurić, M., Ivezić, Ž., Brooks, A., et al. 2008, ApJ, 673, 864
Kirkpatrick, J. D., Henry, T. J., & McCarthy, Jr., D. W. 1991, ApJS, 77, 417
Kleinman, S. J., Kepler, S. O., Koester, D., et al. 2013, ApJS, 204, 5
Kouwenhoven, M. B. N., Goodwin, S. P., Parker, R. J., et al. 2010, MNRAS, 404, 1835
Kraus, A. L., & Hillenbrand, L. A. 2007a, AJ, 134, 2340
—. 2007b, ApJ, 662, 413
—. 2009a, ApJ, 704, 531
—. 2009b, ApJ, 703, 1511
Laughlin, G., Bodenheimer, P., & Adams, F. C. 1997, ApJ, 482, 420
Law, N. M., Dhital, S., Kraus, A., Stassun, K. G., & West, A. A. 2010, ApJ, 720, 1727
Lawrence, A., Warren, S. J., Almaini, O., et al. 2007, MNRAS, 379, 1599
Lépine, S., & Bongiorno, B. 2007, AJ, 133, 889
Lépine, S., & Scholz, R.-D. 2008, ApJ, 681, L33
Lupton, R., Gunn, J. E., Ivezić, Z., et al. 2001, in Astronomical Society of the Pacific Conference Series, Vol. 238, Astronomical Data Analysis Software and Systems X, ed. F. R. Harnden Jr., F. A. Primini, & H. E. Payne, 269
Michell, J. 1767, Royal Society of London Philosophical Transactions Series I, 57, 234
Moeckel, N., & Bate, M. R. 2010, MNRAS, 404, 721
Moeckel, N., & Clarke, C. J. 2011, MNRAS, 415, 1179
Munn, J. A., Monet, D. G., Levine, S. E., et al. 2004, AJ, 127, 3034
—. 2008, AJ, 136, 895
Öpik, E. 1924, Publications of the Tartu Astrofizica Observatory, 25, 1
Padmanabhan, N., Schlegel, D. J., Finkbeiner, D. P., et al. 2008, ApJ, 674, 1217
Pier, J. R., Munn, J. A., Hindsley, R. B., et al. 2003, AJ, 125, 1559
Press, W. H., Teukolsky, S. A., Vetterling, W. T., & Flannery, B. P. 1992, Numerical Recipes in FORTRAN. The Art of Scientific Computing, 2nd edn. (Cambridge: Cambridge Univ. Press)
Radigan, J., Lafrenière, D., Jayawardhana, R., & Doyon, R. 2009, ApJ, 698, 405
Reid, I. N., & Gizis, J. E. 1997, AJ, 113, 2246

Reid, I. N., Hawley, S. L., & Gizis, J. E. 1995, AJ, 110, 1838
Reipurth, B., & Clarke, C. 2001, AJ, 122, 432
Reipurth, B., & Mikkola, S. 2012, Nature, 492, 221
Savcheva, A. S., West, A. A., & Bochanski, J. J. 2014, ApJ, 794, 145
Schlegel, D. J., Finkbeiner, D. P., & Davis, M. 1998, ApJ, 500, 525
Schmidt, S. J., West, A. A., Hawley, S. L., & Pineda, J. S. 2010, AJ, 139, 1808
Schuler, S. C., Cunha, K., Smith, V. V., et al. 2011, ApJ, 737, L32
Sesar, B., Ivezić, Ž., & Jurić, M. 2008, ApJ, 689, 1244
Stassun, K. G., Mathieu, R. D., Cargile, P. A., et al. 2008, Nature, 453, 1079
Stassun, K. G., Mathieu, R. D., & Valenti, J. A. 2007, ApJ, 664, 1154
Terziev, E., Law, N. M., Arcavi, I., et al. 2013, ApJS, 206, 18
Tobin, J. J., Hartmann, L., Looney, L. W., & Chiang, H.-F. 2010, ApJ, 712, 1010
Weinberg, M. D., Shapiro, S. L., & Wasserman, I. 1987, ApJ, 312, 367
West, A. A., Hawley, S. L., Bochanski, J. J., et al. 2008, AJ, 135, 785
West, A. A., Walkowicz, L. M., & Hawley, S. L. 2005, PASP, 117, 706
West, A. A., Hawley, S. L., Walkowicz, L. M., et al. 2004, AJ, 128, 426
West, A. A., Morgan, D. P., Bochanski, J. J., et al. 2011, AJ, 141, 97
White, R. J., & Ghez, A. M. 2001, ApJ, 556, 265
White, R. J., Ghez, A. M., Reid, I. N., & Schultz, G. 1999, ApJ, 520, 811
Wright, E. L., Eisenhardt, P. R. M., Mainzer, A. K., et al. 2010, AJ, 140, 1868
York, D. G., Adelman, J., Anderson, Jr., J. E., et al. 2000, AJ, 120, 1579